

Structure-Phase States of Al-Si Alloy after Electron-Beam Treatment and Multicycle Fatigue

Krestina V. Alsaraeva, Victor E. Gromov, Sergey V. Konovalov, Anna A. Atroshkina

Abstract—Processing of Al-19.4Si alloy by high intensive electron beam has been carried out and multiple increases in fatigue life of the material have been revealed. Investigations of structure and surface modified layer destruction of Al-19.4Si alloy subjected to multicycle fatigue tests to fracture have been carried out by methods of scanning electron microscopy. The factors responsible for the increase of fatigue life of Al-19.4Si alloy have been revealed and analyzed.

Keywords—Al-19.4Si alloy, high intensive electron beam, multicycle fatigue, structure.

I. INTRODUCTION

FATIGUE failure of parts is one of the most commonly occurring causes of equipment, machinery, vehicles and structure failure.

It is due to the specific nature of multicycle fatigue phenomenon consisting in: first, the crack nucleation and development at relatively low stresses; second, the high sensitivity of fatigue life to design, technological and operational factors; third, multiple spread of fatigue life characteristics (spread of fatigue life value) compared to characteristics of static strength; fourth, the local and selective feature of crack nucleation and development without the manifestation of visible residual displacements up to the moments of emergencies [1]. Therefore the problem of preventing the fatigue failures (service life increase) of critical parts is a very important one, especially in the branches of industry where the occurrence of emergencies leads to disastrous consequences. As a rule, fatigue cracks are initiated in the surface layer of the part [2]. Therefore, the state of the surface layer affects significantly the fatigue life of the material.

Application of surface hardening methods results in the appreciable increase of fatigue limit in some cases (by 2-3 times and more), which is connected with the removal of microirregularities (notches, scratches, roughness) of machining, the formation of compressive residual stresses in the surface layer of the hardened parts, the dispersion of matrix structure and inclusions of the second phases [3]. The principal increase of the service properties of material surface

layers is possible providing the purposeful formation of the additional levels of structure-phase state in submicron and nanosize region of their existence in the surface layer. The effective method of this modification and as a consequence, fatigue life increase is the processing of material surface by high intensity electron beam of submillisecond effect duration allowing to change the surface layer structure tens of micrometers thick transforming it into multimodal structure-phase state and essentially without changing the structure-phase state of the alloy basic volume [4]–[12].

Alloys of aluminium with silicon having the high specific mechanical properties are the brittle and difficultly deformed materials. In papers [13]–[22] the structure and phase composition of aluminium alloys are widely investigated. It is necessary to improve essentially their structure and increase the plastic properties for expanding the spheres of these alloys application in aircraft, automobile building and other branches of industry.

It is known that the processing of aluminium alloys' surface by laser radiation may result in the substantial structural changes – the dispersing of structural components, the formation of metastable phases and defects of crystal structure, etc. that result in the improvement of physico-chemical properties of the material [23]–[26]. Besides laser processing the effective tool of high-speed thermal treatment of aluminium alloys' surface is high intensity pulsed electron beams [27]–[31].

The aim of this work is to analyze the regularities of structure modification of Al-19.4Si alloy by high intensity pulsed electron beam, to identify the mechanisms responsible for Al-19.4Si alloy failure subjected to multicycle fatigue tests.

II. MATERIALS AND PROCEDURE

Al-19.4Si alloy (Al – 81, Si – 19.4, Fe – 0.56, wt. %) was used as a material for studies [3]. Fatigue tests were carried out in a special unit on the principle of asymmetric cyclic cantilever bending [32]. Test specimens were in the form of a parallelepiped with dimensions of 8x14x145 mm. The imitation of a crack was done by the semicircle notch of 10 mm radius. Test temperature was 300 K, frequency of specimen loading by bending was 15 Hz under the load of 10 MPa.

Specimen surface irradiation prepared for fatigue tests was carried out using the unit “SOLO” [8] with the following parameters: electron energy = 16 keV; pulse repetition frequency = 0.3 sec⁻¹; pulse duration of the electron beam $\tau =$

V.E. Gromov, K.V. Alsaraeva and S.V. Konovalov are with the Department of Physics, Siberian State Industrial University, Novokuznetsk, 654007 Russia (corresponding author phone: 384-378-4367; fax: 384-346-5792; e-mail: alsaraeva_kv@physics.sibsiu.ru, gromov@physics.sibsiu.ru, konovalov@physics.sibsiu.ru).

A.A. Atroshkina is with the Department of Foreign Language, Siberian State Industrial University, Novokuznetsk, 654007 Russia (e-mail: atrosh2@mail.ru).

50 μs and 150 μs ; pulse number $n = 1, 3, 5$; energy density of electron beam of $E_S = 10, 15, 20, 25 \text{ J} \cdot \text{cm}^{-2}$.

The electron beam energy density varied upon Al-19.4Si alloy surface processing by the electron beam whose energy density was measured by a microcalorimeter placed into the chamber of the "SOLO" device before material irradiation in electron beam testing. The specimen face that is the face above the notch imitating a crack was irradiated. At least 5 specimens were tested for each regime of irradiation. Studies of failure surface were done by methods of scanning electron microscope (Tesla BS-301 microscope).

III. RESULT OF STUDIES AND DISCUSSION

The characteristic failure of Al-19.4Si alloy is the presence of a large number of initial silicon crystallites mainly the plate shaped ones (Fig. 1). The plates are located randomly or decorate the grain boundaries of the alloy. The plate sizes of Al-19.4Si alloy in the plane of metallographic section vary from a few to tens of micrometers. It is apparent that the material containing such an amount of brittle inclusions of different shapes and sizes will have greater spread characteristics of fatigue life.

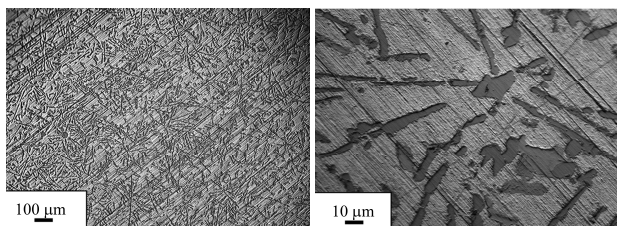


Fig. 1 Al-19.4Si alloy structure before fatigue testing. Metallography of etched metallographic section

In fact, the fatigue tests carried out by us have revealed a wide set of results and essentially depend on both the specimen structure and regime of its irradiation (Fig. 2).

For structural studies of Al-19.4Si alloy surface processing and surface failure the specimens showing the minimal (regimes of irradiation – 15 $\text{J} \cdot \text{cm}^{-2}$; 150 μs ; 3 pulses and 20 $\text{J} \cdot \text{cm}^{-2}$; 150 μs ; 1 pulse) and the maximum (regime of irradiation – 20 $\text{J} \cdot \text{cm}^{-2}$; 150 μs ; 5 pulses) fatigue life were selected.

As mentioned above, fatigue life of the material depends significantly on the of the surface layer structure of the test specimen. Fig. 3 presents the results of the structure studies of Al-19.4Si alloy specimen surface subjected to electron beam irradiation according to regime 15 $\text{J} \cdot \text{cm}^{-2}$; 150 μs ; 3 pulses, this specimen showed the minimal durability under fatigue tests. The analysis of the structure being formed in Al-19.4Si alloy irradiation according to the given regime gives grounds to make a conclusion that electron beam processing results in only partial melting of redundant silicon (Fig. 3 (a)). The process of partial plate melting is accompanied by the formation of numerous micropores located along the plate/matrix interface and microcracks located in the plates (Fig. 3 (b)). Silicon plates are stress concentrators. Fatigue

tests result in plate failure and formation of extended microcracks (Figs. 3 (c) and (d)). Thus, Al-19.4Si alloy surface irradiation by high intensity pulsed electron beam in the regime of melting of redundant silicon inclusions is accompanied by the formation of micropores and microcracks weakening the material in surface layer. It is the crucial factor contributing to a slight increase (see Fig. 2) to fatigue life of the material.

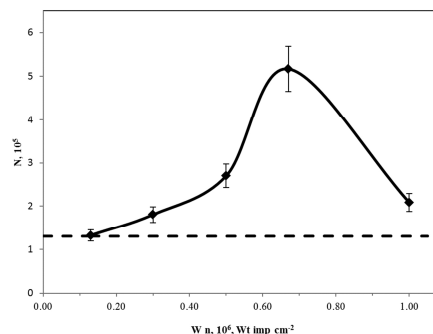


Fig. 2 Dependence of an average (averaging performed on five samples) number of cycles N to failure of Al-19.4Si alloy on the product of the W_S energy density and the number of pulses of n electron beam treatment. The values of fatigue life of the initial material are shown by the dotted line

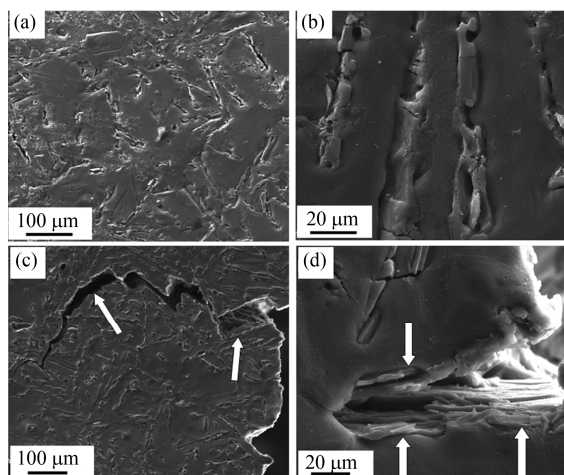


Fig. 3 Al-19.4Si alloy surface structure processed by the electron beam (15 $\text{J} \cdot \text{cm}^{-2}$, 150 μs ; 3 pulses); (a), (b) – the state before fatigue testing; (c), (d) – the state after fatigue testing. Arrows in (c) point to the crack that formed in fatigue testing; in (d) – silicon plates, destroyed in testing

The distinctive images of structures being formed in Al-19.4Si alloy irradiation by high-intensity pulsed electron beam according to regime 20 $\text{J} \cdot \text{cm}^{-2}$; 150 μs ; 5 pulses, showing the maximum fatigue life in tests are shown in Figs. 4 (a) and (b). It shows clearly that surface layer structure differs principally on the basis of morphological features from the initial specimen (Fig. 1) and the specimen irradiated according to regime 15 $\text{J} \cdot \text{cm}^{-2}$ regime; 150 μs ; 3 pulses (Fig. 3). On the irradiation surface the homogeneous structure of the grain

(cellular) type (the grains size of the eutectic ranges from $30\ \mu\text{m}$ to $50\ \mu\text{m}$) is formed. Grains are separated by silicon interlayers the transverse sizes of which do not exceed $20\ \mu\text{m}$ (Fig. 4 (b)). Stress concentrators that can be sources of specimen failure are not detected on the edge of the fracture (Fig. 4 (c)). The cracks parallel to the fracture surface are located at some distance from it (Fig. 4 (d)). It, evidently, indicates that the concentrator being the cause of the specimen failure was located under the surface, most probably, on the interface of the liquid and solid phases.

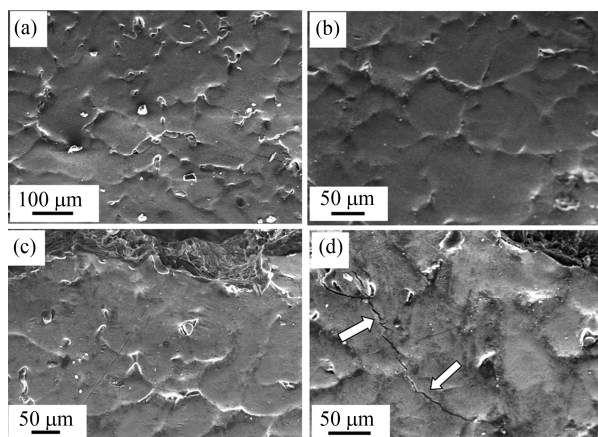


Fig. 4 Al-19.4Si alloy surface structure processed by the electron beam ($20\ \text{J} \cdot \text{cm}^{-2}$, $150\ \mu\text{s}$; 5 pulses); (a), (b) the state before fatigue testing; (c), (d) state after fatigue testing. Arrows in (d) show a microcrack formed in fatigue testing

Thus, the analysis of Al-19.4Si alloy surface irradiated by high-intensity pulsed electron beam has shown that high-speed melting and subsequent surface layer crystallization with the formation of a cellular type structure with distributed interlayers of redundant silicon along the cell boundaries, make possible to increase fatigue life of Al-19.4Si alloy on average by more than 3.5 times relative to the initial state (Fig. 2).

As a rule, fatigue failure is a process developing in time in local volumes of the material. When reaching a certain critical state the destruction of specimen occurs as a whole. On the surface of failure three distinctive zones appear – the zone of fatigue crack growth, the zone of finish breaking and the zone of accelerating crack growth which separates the first two zones [33], [34]. The deformation processes taking place in fatigue testing of the material develop in full measure in the zone of fatigue crack growth and, to a much lesser extent, in the zone of finish breaking. The characteristic image of surface failure of Al-19.4Si alloy specimens destructed in irradiations regimes – $15\ \text{J} \cdot \text{cm}^{-2}$, $150\ \mu\text{s}$; 3 pulses and $20\ \text{J} \cdot \text{cm}^{-2}$, $150\ \mu\text{s}$; 5 pulses, is shown in Fig. 5. Width of fatigue crack growth zone in test Al-19.4Si alloy specimens correlates and is connected with the cycle number before failure, i.e. it depends on the regime of electron beam irradiation of the material. The performed studies have shown that the thickness of fatigue crack growth zone in the specimen destructed in the

regime $15\ \text{J} \cdot \text{cm}^{-2}$; $150\ \mu\text{s}$; 3 pulses was $0.96\ \text{mm}$, but that in the specimen destructed in the regime $20\ \text{J} \cdot \text{cm}^{-2}$; $150\ \mu\text{s}$; 5 pulses was $3.45\ \text{mm}$ (Fig. 5).

Width of fatigue crack growth zone is equated to a critical crack length [1]. Therefore, in optimal irradiation regime of Al-19.4Si alloy surface by electron beam it is possible to increase the critical crack length by more than three times, thereby increasing the service life and efficiency of the material. Similar results were obtained in multicycle loading of ferrite-pearlite steel 60GS2 after electropulsing processing at a certain stage of loading [35], [36].

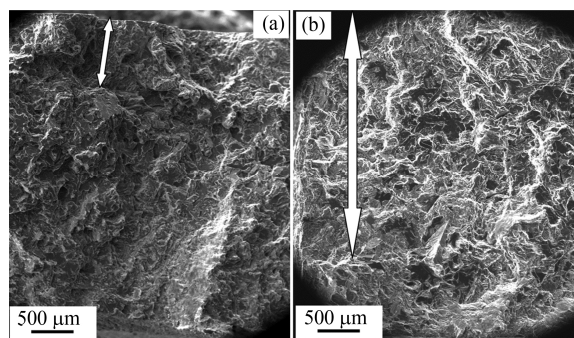


Fig. 5 Surface failure structure of Al-19.4Si alloy specimens irradiated by the electron beam; (a) – regime of irradiation – $15\ \text{J} \cdot \text{cm}^{-2}$; $150\ \mu\text{s}$; 3 pulses; (b) – regime of irradiation – $20\ \text{J} \cdot \text{cm}^{-2}$; $150\ \mu\text{s}$; 5 pulses. Arrows point to the zone of fatigue crack growth

From the value of ratio of fatigue zone area to finish breaking zone it is possible to judge the value of safety coefficient of the material: the lower the ratio, the lower the safety coefficient at the same loading value of fatigue tests [1]. The fractograph analysis of the material under study showed that the value of this coefficient varied from 0.24 ($15\ \text{J} \cdot \text{cm}^{-2}$, $150\ \mu\text{s}$; 3 pulses) to 0.86 ($20\ \text{J} \cdot \text{cm}^{-2}$, $150\ \mu\text{s}$; 5 pulses). Consequently, Al-19.4Si alloy irradiation in optimal regime increases substantially the safety coefficient of material service.

In fatigue tests the cracks are initiated, as a rule, on the specimen surface or in the near-surface layer. Structural analysis of surface layer of Al-19.4Si alloy specimens that showed a relatively low level of fatigue life (in irradiation regimes – $15\ \text{J} \cdot \text{cm}^{-2}$; $150\ \mu\text{s}$; 3 pulses and $20\ \text{J} \cdot \text{cm}^{-2}$; $150\ \mu\text{s}$; 1 pulse) enabled to reveal the source of the material failure. As expected, the large silicon plates located on the surface (Figs. 3 (c) and (d)) and in the near-surface layer (Figs. 6 (a) and (b)) of the specimen were the concentrator of critical stress. In Al-19.4Si alloy surface irradiation by the electron beam according to the regime $20\ \text{J} \cdot \text{cm}^{-2}$; $150\ \mu\text{s}$; 5 pulses the surface layer not less than $20\ \mu\text{m}$ thick melts (Fig. 6 (c)). High-speed crystallization results in the formation of structure the crystallite sizes of which vary from $100\ \text{nm}$ to $250\ \text{nm}$ (Fig. 6 (d)). It is apparent, that the formation of such submicro- and nanosize structure is the primary cause contributing to multiple increase of Al-19.4Si alloy fatigue life.

The appreciable and strongly localized plastic deformation takes place in every cycle of the load changing at the crack tip.

Polycrystalline nature of the structure (the grain structure of solid solution on aluminum basis and a large number of relatively large plates of initial silicon) results in the multiple branching of material failure front. A large number of microscopically visible traces of failure are located in parallel that is especially typical for specimens with the maximum number of cycles before failure (Fig. 5 (b)).

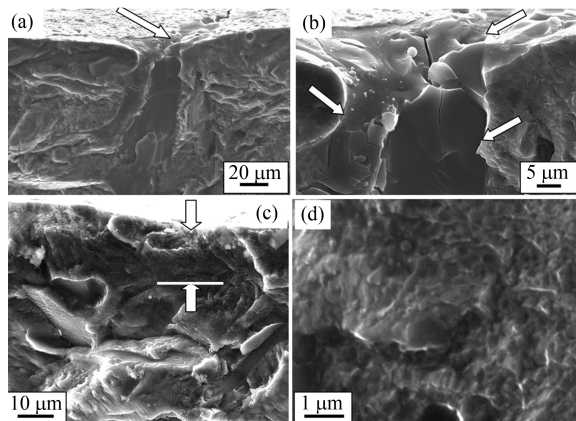


Fig. 6 Electron microscope image of the Al-19.4Si alloy surface fatigue fracture in regimes of irradiation – $20 \text{ J} \cdot \text{cm}^{-2}$; $150 \mu\text{s}$; 1 pulse (a), (b) and $20 \text{ J} \cdot \text{cm}^{-2}$; $150 \mu\text{s}$; 5 pulses (c), (d). Arrows in (a), (b) show to silicon plates; in (c) thickness of Al-19.4Si alloy layer melted by the electron beam

The important failures of fatigue failure zone of the material are fatigue striations; their distinctive image is shown in Fig. 7 [1], [2], [33], [34]. It is known that the term "fatigue striations" means the strips of depressions and asperities consecutively located strips with steps of stress decrease restricted by these depressions located in parallel to crack front. With each cycle of loading a crack (fracture) moves ahead for a definite distance. As this take place, a number of successive strips remain on the surface of failure. It follows that the strips are the trace of crack moving at one space for one cycle of loading. According to Schmidt-Thomas and Klingele these strips are called fatigue striations [36]. They are perpendicular or nearly perpendicular to the directions of crack propagation. The striations may be continuous and regular (typical for aluminum alloys) with decreasing distance between them as the level of stresses is decreased and speed of crack propagation as well. The striations may be discontinuous and irregular that is typical for steel surface failure.

All conditions being equal, the distance between the striations is determined by the ability of the material to resist the fatigue crack propagation: the less the distance between the striations, the more resistant is the material to crack propagation. Our studies have shown that the average distances between the fatigue striations in the Al-19.4Si alloy specimens failed in irradiation regime $15 \text{ J} \cdot \text{cm}^{-2}$; $150 \mu\text{s}$; 3 pulses and $20 \text{ J} \cdot \text{cm}^{-2}$; $150 \mu\text{s}$; 1 pulse are close and on the average equal $0.95 \mu\text{m}$, but in the specimen failed in m irradiation regime $20 \text{ J} \cdot \text{cm}^{-2}$; $150 \mu\text{s}$; 5 pulses they equal $0.28 \mu\text{m}$. Consequently, a spacing of crack for one cycle of

fatigue loading in Al-19.4Si alloy specimen processed according to optimal regime is less by 3.5 times, it follows that this specimen has a higher resistance to fatigue crack propagation.

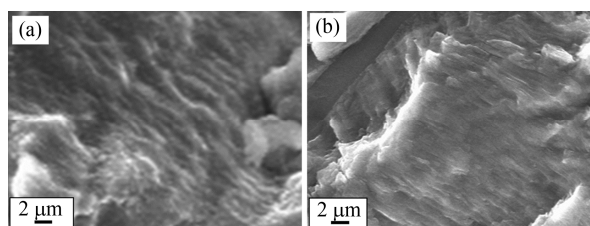


Fig. 7 Fatigue striations being formed in Al-19.4Si alloy as a result of fatigue failure; (a) – specimen failed in regime of irradiation – $20 \text{ J} \cdot \text{cm}^{-2}$; $150 \mu\text{s}$; 1 pulse; (b) – specimen failed in regime of irradiation – $20 \text{ J} \cdot \text{cm}^{-2}$; $150 \mu\text{s}$; 5 pulses

Failure surface, as a rule, has a complex structure. In two-phase materials, to which the analyzed alloy belongs, the mixed mechanism of fatigue failure is used. The analysis of the photos in Fig. 8 reveals the pits of ductile fracture and facets of a quasi-cleavage. Pits are the predominant element of the fracture surface structure and they are formed as a result of cutting the micropores through which the destruction of aluminium grains occurred (Fig. 8 (a)). Silicon plates are destructed according to the cleavage mechanism (Fig. 8 (b)).

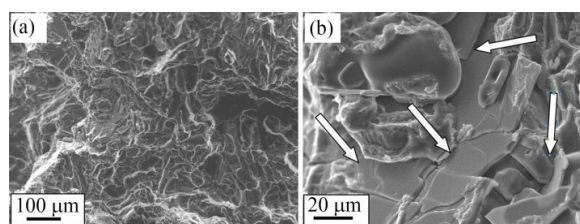


Fig. 8 Electron microscope image of the Al-19.4Si alloy fatigue failure surface (in regime of irradiation – $20 \text{ J} \cdot \text{cm}^{-2}$; $150 \mu\text{s}$; 1 pulse). Arrows in b show silicon plates

IV. CONCLUSION

Surface modification of Al-19.4Si alloy by high intensity pulsed electron beam has been done, the multicycle fatigue tests have been carried out and the irradiation regime permitting the increase of material fatigue life by more than 3.5 times has been identified. It has been shown that the main reasons for Al-19.4Si alloy fatigue life increase are: the considerable increase of the critical crack length, the safety coefficient, and the reduction of average distance between fatigue striations (cracks for cycle loading), the formation of submicro- and nanosize structure.

ACKNOWLEDGMENT

This work was supported by a grant of the RF President for state support of young Russian scientists - doctors (MD-2920.2015.8 project) and state task № 3.1496.2014 / K.

REFERENCES

- [1] G. S. Kocanda, *Fatigue failure of metals*, Alphen aan den Rijn: Sijthoff & Noordhoff International Publishers, 1978.
- [2] J. A. Fellows, "Fractography and Atlas of Fractographs", in *Metals Handbook*, vol. 9, Amer. Soc. Metals, 1974.
- [3] G. B. Stroganov, V. A. Rothenberg and G. B. Gershman, "Aluminum-silicon alloy", Moscow: Metallurgy, 1977.
- [4] Y. F. Ivanov, N. N. Koval, S. V. Gorbunov, S. V. Vorobyov, S. V. Konovalov and V. E. Gromov, "Multicyclic fatigue of stainless steel treated by a high-intensity electron beam: surface layer structure", *Rus. Phys. J.*, vol. 54, pp. 575-583, Oct. 2011.
- [5] V. A. Grishunin, V. E. Gromov, Yu. F. Ivanov, A. D. Teresov and S. V. Konovalov, "Evolution of the phase composition and defect substructure of rail steel subjected to high-intensity electron-beam treatment", *J. of Surf. Investigation. X-ray, Synchrotron and Neutron Techniques*, vol. 7, pp. 990-995, Sept. 2013.
- [6] V. V. Sizov, V. E. Gromov, Y. F. Ivanov, S. V. Vorob'ev and S. V. Konovalov, "Fatigue failure of stainless steel after electron-beam treatment", *Steel in Translation*, vol. 42, pp. 486-488, June 2012.
- [7] Yu. F. Ivanov, D. A. Bessonov, S. V. Vorob'ev, V. E. Gromov, K. V. Ivanov, Yu. A. Kolubaeva and V. Ya. Tsellermaer, "On the fatigue strength of grade 20Cr13 hardened steel modified by an electron beam", *J. of Surf. Investigation. X-ray, Synchrotron and Neutron Techniques*, vol. 7, pp. 90-93, Jan. 2013.
- [8] D. I. Proskurovsky, V. P. Rotshtein, G. E. Ozur, Yu. F. Ivanov and A. B. Markov, "Physical foundations for surface treatment of materials with low energy, high current electron beams", *Surf. and Coat. Technol.*, vol. 125, pp. 49-56, March 2000.
- [9] Yu. F. Ivanov, T. Yu. Kobzareva, S. V. Raikov, V. E. Gromov, N. A. Soskova and E. A. Budovskikh, "Modification of the surface of the VT6 alloy by plasma of electric explosion of a conducting material and by electron beam", *Russian J. of Non-Ferr. Met.*, vol. 55, pp. 51-56, Jan. 2014.
- [10] S. Z. Hao, Y. Qin, X. X. Mei, B. Gao, J. X. Zuo, Q. F. Guan, C. Dong and Q. Y. Zhang, "Fundamentals and applications of material modification by intense pulsed beams", *Surf. and Coat. Technol.*, vol. 201, pp. 8588-8595, August 2007.
- [11] J. J. Hu, G. B. Zhang, H. B. Xu and Y. F. Chen, "Microstructure characteristics and properties of 40Cr steel treated by high current pulsed electron beam", *Mater. Sci. and Technol.*, vol. 27, pp. 300-303, April 2012.
- [12] L. J. Tan, Z. K. Yao, T. Wang and H. Z. Guo, "Effect of post-weld heat treatment on microstructure and properties of electron beam welded joint of Ti2AlNb/TC11", *Mater. Sc. and Technol.*, vol. 27, pp. 1315-1320, August 2011.
- [13] M. Elmadagli, T. Perry and A. T. Alpas, "A parametric study of the relationship between microstructure and wear resistance of Al-Si alloys", *Wear*, vol. 262, pp. 79-92, Jan. 2007.
- [14] M. Zeren and E. Karakulak, "Influence of Ti addition on the microstructure and hardness properties of near-eutectic Al-Si alloys", *J. of Alloys and Compounds*, vol. 450, pp. 255-259, February 2008.
- [15] C. X. Guang and E. Siegfried, "Einfluss des wasserstoff-fanporositat Al-Si and Al-Mg legierungen", *Giesserei*, vol. 78, pp. 679-684, 1990.
- [16] R. C. Hernandez and J. H. Sokolowski, "Thermal analysis and microscopical characterization of Al-Si hypereutectic alloys", *J. of Alloys and Compounds*, vol. 419, pp. 180-190, August 2006.
- [17] M. Zeren, "The effect heat-treatment on aluminum-based piston alloys", *Materials and design*, vol. 28, 2511-2517, 2007.
- [18] R. Taghiabadi, H. M. Ghasemi and S. G. Shabestari, "Effect of iron-rich intermetallics on the sliding wear behavior of Al-Si alloys", *Mater. Sci. and Engineering A*, vol. 490, pp. 162-167, August 2008.
- [19] R. X. Li, R. D. Li, L. Z. He, C. X. Li, H. R. Gruan and Z. Q. Hu, "Age-hardening behavior of cast Al-Si base alloy", *Materials Letters*, vol. 58, pp. 2096-2101, June 2004.
- [20] N. A. Belov, D. G. Eskin and A. A. Aksenov, *Multicomponent Phase Diagrams: Applications for Commercial Aluminum Alloys*, Amsterdam: Elsevier, 2005.
- [21] N. A. Belov, D. G. Eskin and N. N. Avxentieva, "Constituent Phase Diagrams of the Al-Cu-Fe-Mg-Ni-Si System and their Application to the Analysis of Aluminium Piston Alloys", *Acta Materialia*, vol. 53, pp. 4709-4722, Oct. 2005.
- [22] A. M. A. Mohamed, A. M. Samuel, F. H. Samuel and H. W. Doty, "Influence of additives on the microstructure and tensile properties of near-eutectic Al-10.8%Si cast alloy", *Materials and Design*, vol. 30, pp. 3943-3957, 2009.
- [23] T. T. Wong and G. Y. Liang, "Effect of Laser Melting Treatment on the Structure and Corrosion Behavior of Aluminium and Al-Si Alloys", *J. of Materials Processing Technology*, vol. 63, pp. 930-934, Jan. 1997.
- [24] E. Sicard, C. Boulmer-Leborgne, C. Andreazza-Vignolle and M. Frainais, "Excimer laser surface treatment of aluminum alloy in nitrogen", *Appl. Phys. A*, vol. 73, pp. 55-60, July 2001.
- [25] P. H. Chong, Z. Liu, P. Skeldon and G. E. Thompson, "Large area laser surface treatment of aluminum alloys for pitting corrosion protection", *Applied Surface Science*, vol. 208-209, pp. 399-404, March 2003.
- [26] S. Tomida, K. Nakata, S. Shibata, I. Zenkouji and S. Saji, "Improvement in wear resistance of hyper-eutectic Al-Si cast alloy by laser surface remelting", *Surf. and Coat. Technol.*, vol. 169-170, pp. 468-471, June 2003.
- [27] J. An, X. X. Shen, Y. Lu and Y. B. Liu, "Microstructure and tribological properties of Al-Pb alloy modified by high current pulsed electron beam", *Wear*, vol. 261, pp. 208-215, July 2006.
- [28] Y. Hao, B. Gao, G. F. Tu, S. W. Li, S. Z. Hao and C. Dong, "Surface modification of Al-20Si alloy by high current pulsed electron beam", *Applied Surface Science*, vol. 257, pp. 3913-3919, Feb. 2011.
- [29] Y. Hao, B. Gao, G. F. Tu, H. Cao, S. Z. Hao and C. Dong, "Surface modification of Al-12.6Si alloy by high current pulsed electron beam", *Applied Surface Science*, vol. 258, pp. 2052-2056, Jan. 2012.
- [30] J. An, X. X. Shen, Y. Lu, Y. B. Liu, R. G. Li, C. M. Chen and M. J. Zhang, "Influence of high current pulsed electron beam treatment on the tribological properties of Al-Si-Pb alloy", *Surf. and Coat. Technol.*, vol. 200, pp. 5590-5597, May 2006.
- [31] Y. Hao, B. Gao, G. F. Tu, Z. Wang and C. Z. Hao, "Influence of high current pulsed electron beam (HCPB) treatment on wear resistance of hypereutectic Al-17.5Si and Al-20Si Alloys", *Materials Science Forum*, vol. 675-677, pp. 693-696, 2011.
- [32] S. V. Konovalov, A. A. Atroshkina, Yu. F. Ivanov and V. E. Gromov, "Evolution of dislocation substructures in fatigue loaded and failed stainless steel with the intermediate electropulsing treatment", *Mater. Sci. and Eng. A*, vol. 527, pp. 3040-3043, May 2010.
- [33] V. S. Ivanova and A. A. Shanyavskii, *Quantitative Fractography. Fatigue Fracture*, Chelyabinsk: Metallurgiya, 1988.
- [34] V. F. Terent'ev, *Fatigue of Metallic Materials*, Cambridge: Cambridge Intern. Science Publ, 2004.
- [35] O. V. Sosnin, V. V. Tsellermaer, Yu. F. Ivanov, V. E. Gromov and É. V. Kozlov, "Evolution of the Structure and Carbon Atom Transfer in the Zone of Fatigue Crack Growth in Ferrite-Pearlite Steel", *Rus. Phys. J.*, vol. 46, pp. 1047-1056, Oct. 2003.
- [36] L. Engel and H. Klingele, *Scanning Electron Microscopy: Fracture*, Munich: Carl Hanser, 1982.